

# Synthesis, DNA-binding and Antibacterial Activity of the Cell-penetrating Peptide HIV-1 Tat (49-57)

M. X. LV<sup>1</sup>, B. C. DUAN<sup>1</sup>, K. LU<sup>1\*</sup>, Y. J. WU<sup>1</sup> AND Y. F. ZHAO<sup>\*</sup>

College of Chemistry and Molecular Engineering, Zhengzhou University, <sup>1</sup>School of Material and Chemical Engineering, Henan University of Engineering, Zhengzhou, Henan, China

Lv, *et al.*: Synthesis, DNA-binding and Antibacterial Activity of Peptide Tat (49-57)

The interaction of cell-penetrating peptide human immunodeficiency virus transacting activator of transcription, peptide Tat (49-57), which is the minimal transduction domain of human immunodeficiency virus Tat protein, with calf thymus DNA was investigated with UV/Vis spectroscopy, fluorescence spectroscopy, circular dichroism, and viscometry. Peptide Tat (49-57) could interact with DNA via the groove binding mode, which is accompanied with electrostatic interaction. The fluorescence experiments revealed that the binding constant was  $2.63 \times 10^5 \text{ l} \times \text{mol}^{-1}$ . The UV/Vis spectroscopy and circular dichroism results revealed that the interaction of Tat (49-57) binding with calf thymus DNA disturbed the acting force of accumulation between DNA base pairs. The antimicrobial study using Tat (49-57) against bacteria proved that Tat (49-57) possessed antimicrobial activity against both Gram-positive and Gram-negative bacteria with low haemolysis.

**Key words:** Human immunodeficiency virus Tat (49-57), synthesis, calf thymus DNA, binding mode, antibacterial activity

Cell-penetrating peptides, also called protein transduction domains (PTDs), are short cation peptides that can traverse the cell membranes<sup>[1-3]</sup>. During their cellular uptake, they can deliver various molecules into cells; these molecules include peptides, proteins, oligonucleotides, and nanoparticles<sup>[4-8]</sup>, most of which otherwise cannot cross the cell membranes by their own. Transacting activator of transcription protein transduction domain (Tat-PTD) is derived from the Tat protein of human immunodeficiency virus (HIV) and is widely used to deliver different molecules into cells with causing non cellular injury and no toxicity<sup>[3, 9, 10]</sup>. The cell-penetrating property of Tat-PTD results from its basic epitope (amino acids 49-57), which is the minimal transduction domain of Tat protein, includes two lysine's and six arginine's within a linear sequence of nine amino acid residues (RKKRRQRRR). Tat (49-57) is a short cationic peptide, possessing a high net positive charge at physiological pH. Recent studies proved that TAT can form transient pores and translocate across the membranes by diffusing on these pores, on account of the strong electrostatic attraction between positively-charged Tat (49-57) and negatively-charged phospholipid<sup>[3, 11]</sup>.

After penetrating the cell membranes, Tat-PTD locates in the cell nucleus<sup>[12, 13]</sup>, and the uptake into the nucleus precedes its digestion<sup>[14]</sup>, thereby suggesting that the intracellular Tat-PTD can bind to DNA. DNA possesses a crucial role in the whole biological process; consequently, DNA becomes a pharmacological target for various kinds of antimicrobial drugs<sup>[15]</sup>. Thus, illuminating the binding mode of Tat-PTD with DNA can help understand the molecular mechanisms of drug action and can provide modification guidelines to enhance the clinical efficacy and bioavailability of Tat-PTD and its derivatives.

High affinity of the peptide Tat for DNA has been investigated<sup>[14]</sup>. However, the binding mode and main type of non-covalent interactions in the binding process between Tat (49-57) and DNA have not yet been illustrated in detail. Therefore, we systematically investigated the binding mode and stability of Tat

This is an open access article distributed under the terms of the Creative Commons Attribution-NonCommercial-ShareAlike 3.0 License, which allows others to remix, tweak, and build upon the work non-commercially, as long as the author is credited and the new creations are licensed under the identical terms

Accepted 08 September 2017

Revised 09 March 2017

Received 01 November 2016

Indian J Pharm Sci 2017;79(6):893-899

\*Address for correspondence

E-mail: lukui126@126.com

November-December 2017

Indian Journal of Pharmaceutical Sciences

893

(49-57) to double-stranded DNA by using various techniques. Furthermore, peptide Tat (49-57) is an Arg-rich cationic peptide that is capable of penetrating the membrane to target nucleus, which indicates the potential of Tat (49-57) as a novel antimicrobial peptide<sup>[6]</sup>; hence, the antimicrobial activities of Tat (49-57) were also tested.

## MATERIALS AND METHODS

Fmoc-Arg (Pbf)-Wang resin, Fmoc-Arg (Pbf)-OH, Fmoc-lys(Boc)-OH, Fmoc-Gln(Trt)-OH, 2-(7-Aza-1H-benzotriazole-1-yl)-1,1,3,3-tetramethyluronium hexafluorophosphate (HATU), N,N-diisopropylethylamine (DIEA), and trifluoroacetic acid (TFA) were purchased from GL Biochem, Shanghai, China. Calf thymus DNA (ct-DNA) was obtained from Sigma Ltd., Shanghai, China, and ethidium bromide (EB) was purchased from Fluka Chemie.

Bacterial strains, including Gram-positive *Staphylococcus aureus* (ATCC 29213), *S. epidermidis* (KCTC 1917) and *Bacillus subtilis* (KCTC 3068) and Gram-negative bacteria *Escherichia coli* (ATCC 25922) and *Salmonella typhimurium* (CMCC 50013) were provided by the School of Biological Engineering, Henan University of Technology.

### Peptide synthesis:

Peptide Tat (49-57) was synthesized in accordance with standard Fmoc solid-phase peptide synthesis procedures<sup>[17]</sup>. The crude peptide was purified by reversed phase high-performance liquid chromatography (HPLC) with a semi-preparative Agilent C<sub>18</sub> column (pore size: 300 Å, partial size: 5 µm, 250 mm×9.4 mm). The buffer system consisted of buffer A: 0.1% (v) TFA in MeCN/H<sub>2</sub>O 10:90 (v/v) and buffer B: 0.1% (v) TFA in MeCN/H<sub>2</sub>O 50:50 (v/v). Gradient elution with buffer A to buffer B in 20 min was used at a rate of 2 ml×min<sup>-1</sup>. The molecular mass of peptide Tat (49-57) was confirmed using LCQ Fleet MS (Thermo Scientific, USA).

### UV spectroscopic method:

UV/Vis spectra were recorded on UV-3600 spectrometer (Shimadzu Corporation, Japan) using quartz cuvettes (10 mm path length). Absorption titration experiments were conducted by maintaining the concentration of ct-DNA (50 µM) and changing the Tat (49-57) concentration. The UV/Vis measurements were carried out after the solutions were equilibrated for 10 min. During absorption measurements, equal

concentration of Tat (49-57) was subtracted to eliminate the background absorption in the range of 190-350 nm.

### Fluorescence measurements:

Fluorescence spectra were recorded in 10 mm quartz cells on a Cary Eclipse spectrofluorometer (Agilent, Australia). EB was used in fluorescence measurements as fluorescence probe. About 3 ml of ct-DNA-EB complex solution containing ct-DNA (50 µM) and EB (5 µM) was constant and titrated with peptide Tat (49-57). The mixtures in all experiments were allowed to stand for 10 min to equilibrate before measurement. Emission spectra were measured in the range of 500-750 nm at the excitation wavelength of 262 nm.

DNA melting studies were carried out via monitoring the fluorescence intensities of DNA-EB and DNA-EB-Tat (49-57) complex at 20-100°. The temperature was monitored by a thermostat attached to the sample holder. The melting temperature ( $T_m$ ) of DNA was determined as the transition midpoint.

### Circular dichroism (CD) studies:

CD measurements were conducted on a Mos-500 spectropolarimeter (Bio-Logic, France). The ct-DNA solution (50 µM) in Tris-HCl buffer (pH 7.4) was titrated with Tat (49-57). Equal concentrations of Tat (49-57) were subtracted from the corresponding spectra of samples. The CD spectra were recorded in the range of 220-320 nm using 10 mm path length cell at 37°.

### Viscosity measurements:

Viscosity measurements were conducted via Ubbelodhe viscometer maintained at 25±0.1° in a thermostat water bath. Different amounts of Tat (49-57) were added to ct-DNA with constant concentration (50 µM). After equilibrium for 15 min, the flow time of samples was measured in triplicate to obtain the concurrent values using a digital stopwatch. The data were presented as  $(\eta/\eta_0)^{1/3}$  versus  $C_{\text{Tat (49-57)}}/C_{\text{DNA}}$ , where  $\eta_0$  and  $\eta$  are the specific viscosity of DNA in the absence and presence of Tat (49-57), respectively.

### Antimicrobial activity test:

Broth microdilution method<sup>[3]</sup> was used to examine the antibacterial activities of Tat (49-57). About 100 µl of Tat (49-57) solution (serial two-fold dilutions in sterile water) was added to 100 µl of bacterial suspension (2×10<sup>4</sup> CFU/ml) in 1% peptone. The medium without bacteria was used as negative control. After incubation at 37° for 20 h, the minimal inhibitory concentration (MIC) was determined.

## Haemolysis activity assay:

Haemolysis activity of Tat (49-57) was tested against human erythrocytes. Human blood was collected in a tube containing heparin sulphate from a healthy volunteer after written informed consent under a protocol approved by Zhengzhou University Life Science Ethics Committee. The fresh blood was centrifuged ( $2000\times g$ , 3 min,  $4^\circ$ ) to collect erythrocytes and subsequently washed with PBS (10 mM phosphate buffer, pH 7.4) for 5 times<sup>[18]</sup>. Serial two-fold dilutions of Tat (49-57) were performed in PBS buffer and added to 4% (v/v) erythrocytes dispensed in 96-well plates. The mixture was incubated at  $37^\circ$  for 30 min. Erythrocytes without Tat (49-57) and 0.1% (v/v) Triton X-100 were employed as negative and positive controls, respectively. The supernatants were obtained, and the absorbance was measured at 570 nm. The hemolysis was calculated using the following Eqn., haemolysis (%) =  $[(A_{\text{Tat (49-57)}} - A_{\text{PBS}}) / (A_{\text{Triton}} - A_{\text{PBS}})] \times 100$ .

## RESULTS AND DISCUSSION

Tat (49-57) was synthesized via solid-phase peptide synthesis procedures on Wang resin and purified through RP-HPLC. The final product was white powder of 97.2% purity and characterized by electrospray ionization mass spectrometry (ESI-MS, fig. 1). The sequence of Tat (49-57) was RKKRRQRRR, and its theoretical molecular weight was  $1339.62 \text{ g}\times\text{mol}^{-1}$ . MS (m/e): 670.50  $[\text{M}+2\text{H}]^{2+}$ , 447.50  $[\text{M}+3\text{H}]^{3+}$ , 336.00  $[\text{M}+4\text{H}]^{4+}$ , 269.08  $[\text{M}+5\text{H}]^{5+}$ , 485.08  $[\text{M}+3\text{K}]^{3+}$  was consistent with the molecular peptide Tat (49-57).

UV/Vis spectroscopy is an effective technique to detect interactions between DNA and small molecules. The mode of the interactions is reflected from the changes in the position of the peak and absorptive intensity<sup>[19]</sup>. The UV spectra of ct-DNA with different concentrations of Tat (49-57) are shown in fig. 2. A slight reduction in the absorption band at 260 nm occurred upon the initial addition of Tat (49-57). Hyperchromism was observed upon the subsequent addition of Tat (49-57) to ct-DNA solution. Hypochromism was due to the electrostatic interaction of DNA phosphate groups with the side chains of Tat (49-57). This interaction tightened the double strands of DNA to prevent aromatic bases from becoming increasingly exposed and resulted in the reduced absorption intensity<sup>[20,21]</sup>. With the increase in the concentration of Tat (49-57), when the groove of ct-DNA was padded by Tat (49-57), the interaction of side chains containing guanidine and amino groups of

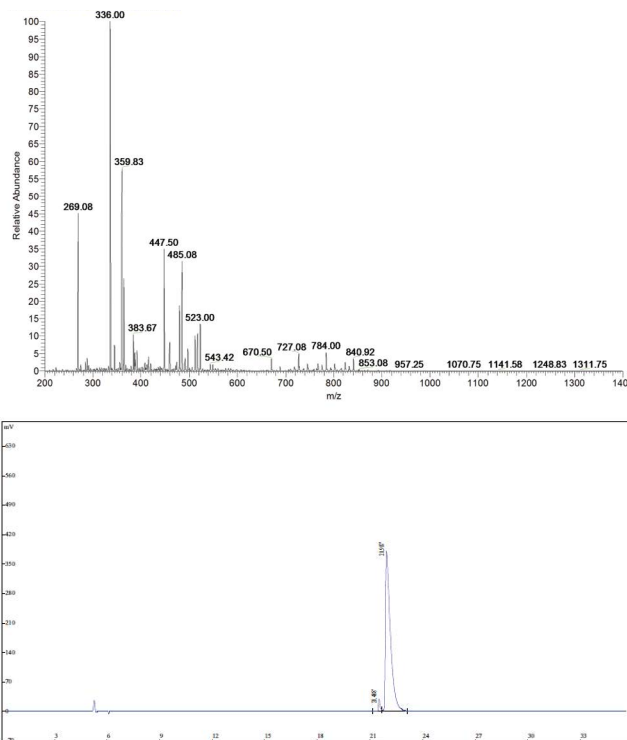


**Fig. 1: Molecular mass and HPLC spectrum of Tat (49-57) (RKKRRQRRR)**

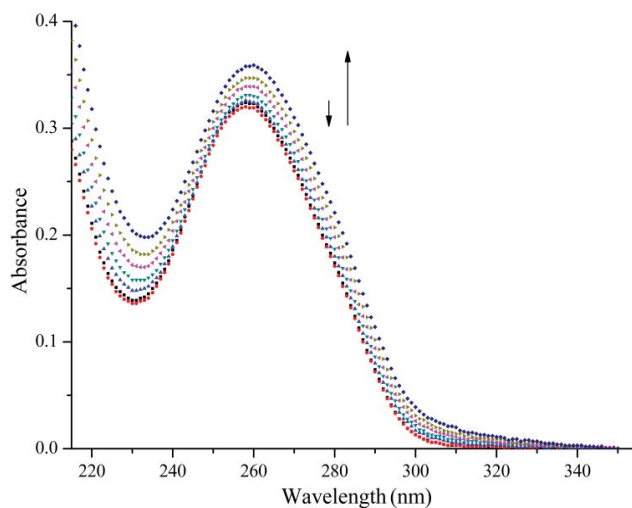


**Fig. 2: Interaction of Tat (49-57) with ct-DNA using UV/Vis spectroscopy**

UV/Vis absorption spectra of ct-DNA (50  $\mu\text{M}$ ) in presence of increasing concentrations of Tat (49-57) (0-6  $\mu\text{M}$ ) in 50 mM Tris-HCl buffer (pH 7.4). Tat (49-57): ■ 0; ● 1; ▲ 2; ▼ 3; ◆ 4; ► 5; ◇ 6

Tat (49-57) destabilized the base pairs of DNA, caused the aromatic bases to become exposed, and resulted in hyperchromism of DNA<sup>[22]</sup>. The structure of Tat (49-57) very closely resembles DNA minor groove binders netropsin<sup>[23,35]</sup>, possessing positive charges and linearity. Therefore, according to the experimental data, minor groove binding interactions might have occurred

between ct-DNA and Tat (49-57), and the interactions of Tat (49-57) with ct-DNA disrupted the accumulative force between DNA base pairs.

Fluorescence probe should be utilized because of the non-fluorescence of Tat (49-57) and the minimal practical usefulness of intrinsic fluorescence from DNA<sup>[24]</sup>. In this work, EB was used as the fluorescence probe. The fluorescence intensity of DNA can be enhanced after interaction with EB because EB can intercalate into the DNA base pairs<sup>[25-27]</sup>.

Fig. 3 shows the fluorescence spectra of ct-DNA-EB with different concentrations of Tat (49-57). The fluorescence intensity at 600 nm weakened remarkably upon the addition of Tat (49-57) to ct-DNA-EB complex. This result suggests that EB in the DNA-EB complex might have been substituted by Tat (49-57) and led to the decrease in fluorescence intensity or a new DNA-EB-Tat (49-57) complex that did not have any fluorescence was formed by Tat (49-57) binding with DNA-EB. The high affinity of EB with DNA was hardly be disrupted by Tat (49-57) because the binding constant ( $2.63 \times 10^5 \text{ l} \times \text{mol}^{-1}$ ) between Tat (49-57) and DNA was lower than that of the classical intercalation binding of DNA-EB complex ( $2 \times 10^6 \text{ l} \times \text{mol}^{-1}$ )<sup>[22]</sup>. Therefore, the formation of non-fluorescence complex DNA-EB-Tat (49-57) was the probable cause of the decrease in the fluorescence intensity of DNA-EB complex. We therefore deduce that the interaction between Tat (49-57) and DNA is not intercalation binding. The quenching mechanism of DNA-EB by Tat (49-57) was analysed with the Stern-Volmer Eqn.,  $F_0/F = 1 + K_q \tau_0 [Q]$ , where, F and  $F_0$  are the fluorescence intensities of DNA-EB system in the presence and absence of Tat (49-57), respectively.  $K_q$  is the quenching rate constant, and Q is the concentration of Tat (49-57).  $\tau_0$  is the average lifetime of fluorophore without Tat (49-57), and its value is approximately  $10^{-8} \text{ s}$ <sup>[28]</sup>.

The quenching type, which can be classified as dynamic quenching and static quenching, was analysed with the Stern-Volmer Eqn.  $K_q$  was obtained from the intercept of the linear of  $F_0/F$  versus Q (fig. 4). For Tat (49-57), the value of  $K_q$  was  $6.41 \times 10^{12} \text{ l} \times \text{mol}^{-1} \times \text{s}^{-1}$ , which was much higher than the value of the maximum scatter collision quenching constant of various quenchers with biomolecules ( $2.0 \times 10^{10} \text{ l} \times \text{mol}^{-1} \times \text{s}^{-1}$ )<sup>[29]</sup>. This finding suggests that the quenching type of Tat (49-57) binding with DNA is static quenching. The binding constant (K) and binding site (n) of Tat (49-57) with the DNA-

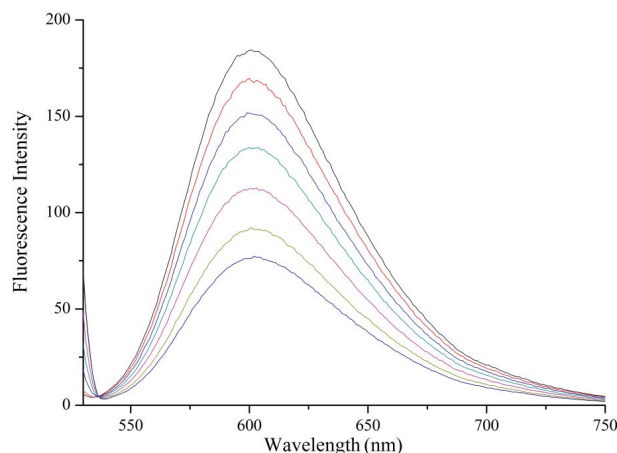


**Fig. 3: Effect of Tat (49-57) on the fluorescence spectra of DNA-EB**

**Fluorescence quenching spectra of DNA-EB ( $C_{\text{DNA}} = 50 \mu\text{M}$ ,  $C_{\text{EB}} = 5.0 \mu\text{M}$ ) upon addition of increasing amount of Tat (49-57); — 0, — 1, — 2, — 3, — 4, — 5, — 6  $\mu\text{M}$**

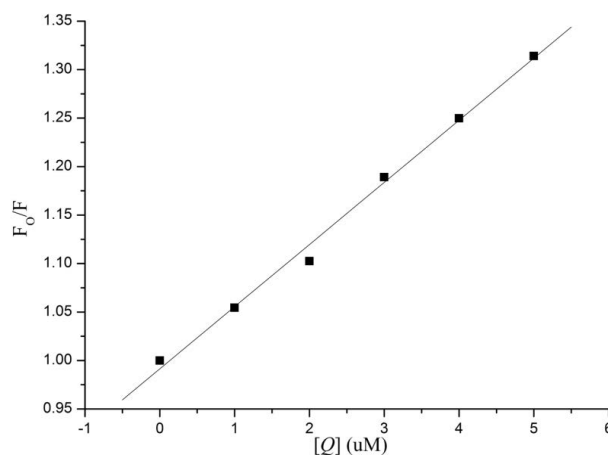


**Fig. 4: The Stern-Volmer plots for the quenching of DNA-EB by Tat (49-57)**

$C_{\text{DNA}} = 50 \mu\text{M}$ ,  $C_{\text{EB}} = 5.0 \mu\text{M}$

EB complex was evaluated with the following Eqn.,  $\log[(F_0 - F)/F] = \log K + n \log [Q]$ .  $\log [(F_0 - F)/F]$  versus  $\log [Q]$  was plotted, and a line with a good linear correlation was obtained (fig. 5). According to this line, binding constant K was determined to be  $2.63 \times 10^5 \text{ l} \times \text{mol}^{-1}$ , and n was 1.12. K was similar to the value that had been well-established among groove binding agents<sup>[30]</sup>.

In this experiment, the melting temperature ( $T_m$ ) was measured with the fluorescence technique. The intercalative binding mode can stabilize the helix structure of DNA and causes the melting temperature to increase by about 5-8°, but the electrostatic and groove binding interactions cause no obvious or minimal change in  $T_m$ <sup>[15,24]</sup>. The melting curves (fig. 6) showed that the  $T_m$  of ct-DNA-EB in the absence

(fig. 6a) of Tat (49-57) was  $87.3 \pm 1^\circ$ , and the  $T_m$  of ct-DNA-EB-Tat (49-57) complex (fig. 6b) was  $85.6 \pm 1^\circ$  under the experimental conditions. The interaction of Tat (49-57) with ct-DNA caused  $T_m$  to decrease. The interaction of Tat (49-57) decreased the stability of ct-DNA double helix structure and affected the affinity of EB with DNA. The change in the  $T_m$  of ct-DNA-EB complex after the addition of Tat (49-57) was less than  $5^\circ$ , revealing that the interaction of Tat (49-57) with DNA is electrostatic or groove binding.

The changes in the secondary structure of DNA during molecule-DNA interactions can be determined through CD spectroscopy<sup>[31]</sup>. The specific CD spectrum of B-form DNA consists of a negative band at 247 nm caused by the right-handed helicity of DNA and a positive band at 275 nm caused by the accumulation of

base pairs<sup>[15]</sup>. The CD spectra of ct-DNA with Tat (49-57) are shown in fig. 7. The positive band at 275 nm decreased remarkably with an apparent red shift, and the band at 245 nm gained slight negativity without a major red shift. The decrease in the positive band at 275 nm indicated that the binding of Tat (49-57) weakened the stacking interactions between base pairs of DNA<sup>[32]</sup>, and the slight increase in the negative band at 245 nm revealed that the interaction of Tat (49-57) with DNA tightened the double helix of DNA. These results are consistent with the UV/Vis spectroscopy results.

The intercalative binding mode generally causes DNA viscosity to increase significantly because

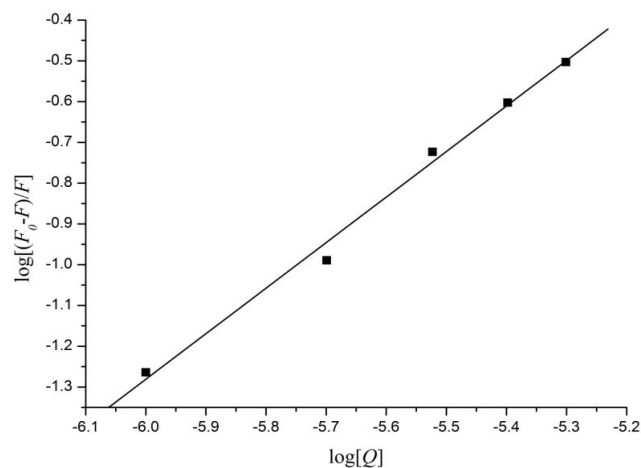


Fig. 5: Plot of  $\log(F_0 - F)/F$  versus  $\log[Q]$

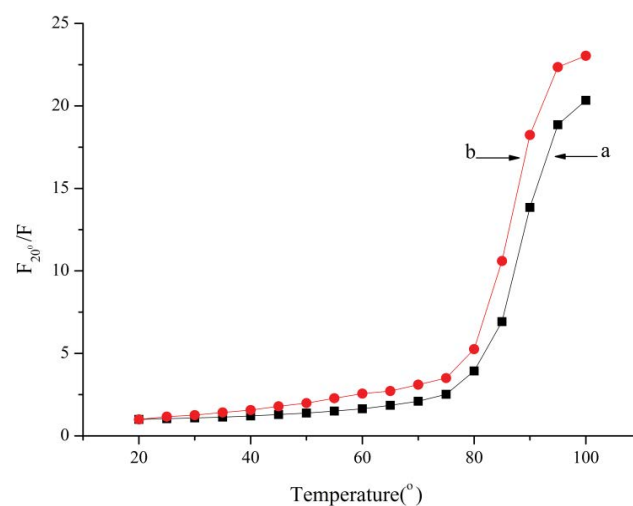


Fig. 6: Effect of Tat (49-57) on the melting temperature of DNA-EB

Melting curves of DNA-EB in the absence (a) and presence (b) of Tat (49-57) ( $C_{DNA} = 50 \mu\text{M}$ ,  $C_{EB} = 5.0 \mu\text{M}$  and  $C_{Tat(49-57)} = 5.0 \mu\text{M}$ )

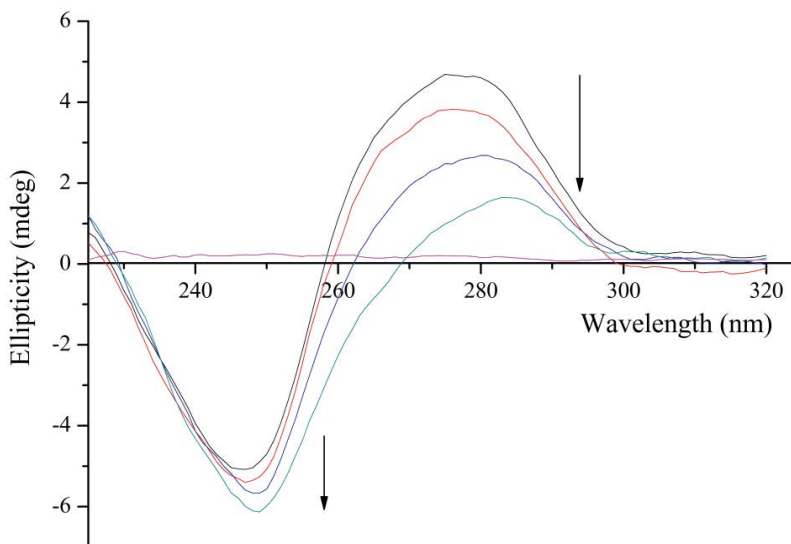
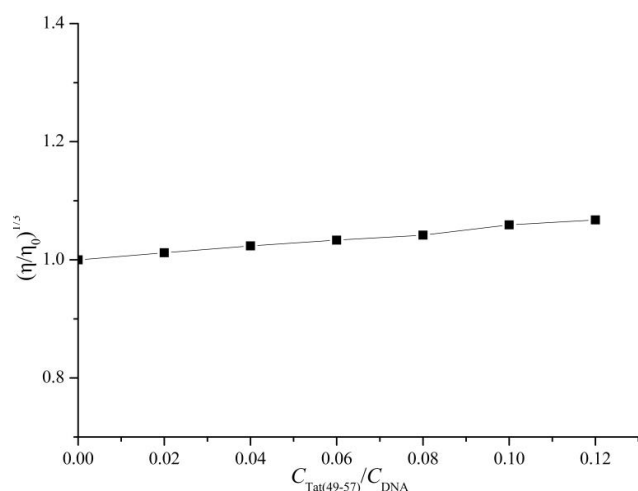


Fig. 7: Effect of Tat (49-57) on CD spectra of ct-DNA

CD spectra of ct-DNA (50  $\mu\text{M}$ ) in 50 mM Tris-HCl (pH 7.4) with varying concentration of Tat (49-57), 0-6  $\mu\text{M}$ . — Free Tat (49-57); — free DNA; — DNA+Tat (49-57), 2  $\mu\text{M}$ ; — DNA+Tat (49-57), 4  $\mu\text{M}$ ; — DNA+Tat (49-57), 6  $\mu\text{M}$

the intercalative mode requires the DNA base pairs to separate sufficiently at intercalative sites to accommodate the binding molecule; this separation increases the effective length of DNA. However, the non-intercalative binding mode causes less change in the viscosity of the DNA solution<sup>[26,30]</sup>. As shown in fig. 8, the viscosities of ct-DNA increased slightly upon continued addition of Tat (49-57); this increase is not as pronounced as that observed in the classical intercalator<sup>[33]</sup> but very similar to distamycin<sup>[34]</sup> a well-known classical DNA minor groove binder. This result confirmed that Tat (49-57) preferred to interact with DNA through groove binding mode rather than classical intercalative interaction.

The broth microdilution method was utilized to measure the antibacterial activities of Tat (49-57). The MIC values of Tat (49-57) against bacterial strains, including two Gram-negative and three Gram-positive species, are summarized in Table 1. Compared with melittin, Tat (49-57) displayed potent antibacterial activity, with the MIC value within the 8-16  $\mu\text{M}$  range.



**Fig. 8: Effect of increasing concentration of Tat (49-57) on viscosity of ct-DNA**  
Concentration of ct-DNA was kept constant (50  $\mu\text{M}$ ) while varying the concentration of Tat (49-57)

**TABLE 1: ANTIMICROBIAL ACTIVITY OF PEPTIDES**

Peptide	MIC ( $\mu\text{M}$ )				
	<i>E. coli</i>	<i>S. typhimurium</i>	<i>B. subtilis</i>	<i>S. epidermidis</i>	<i>S. aureus</i>
Tat (49-57)	8.04±0.08	16.12±0.08	15.93±0.10	8.07±0.17	16.25±0.12
Melittin	2.13±0.13	4.15±0.18	2.02±0.12	1.97±0.13	1.96±0.25

Each value of antimicrobial activity is expressed as the mean±SD of three independent experiments. MIC was determined from three independent experiments performed in triplicate

**TABLE 2: HEMOLYTIC ACTIVITY OF PEPTIDES**

Peptides ( $\mu\text{M}$ )	256	128	64	32	16	8	4	2
Tat (49-57)	4.16	3.29	1.88	1.41	0.47	0	0	0
Melittin	100	100	100	100	98	91	92	68

We also examined the haemolytic activity of Tat (49-57) against human erythrocytes. It did not show haemolysis of human erythrocytes in all the tested concentrations (Table 2). The side chains of Tat (49-57) have two cationic tail groups (guanidine). The structural features of Tat (49-57) are similar to head-to-head pyrrole tetraamides<sup>[34,35]</sup>, that can display antibacterial activity and also bind to the minor groove of DNA. Several other studies also revealed that agents that can bind to DNA.

In the proposed study, the interaction between Tat (49-57) and ct-DNA was studied through UV/Vis spectroscopy, fluorescence spectroscopy, CD spectroscopy and viscosity measurements. The results indicated that Tat (49-57) can bind to DNA through minor groove binding. The results were supported by competitive binding assay with EB, DNA melting, and viscosity measurement studies. Tat (49-57, RKKRRQRRR) is an Arg-rich peptide, similar to Q/RGR-motif peptides<sup>[36]</sup>. Its side chains have the first and last residues (R). Tat (49-57) may directly contact the minor groove of AT-rich sequences via inserting guanidine and amino groups from Tat (49-57) side chains into the minor groove. Tat (49-57) also displayed antibacterial activity, with an MIC value within the 8-16  $\mu\text{M}$  range; it showed no haemolysis of human erythrocytes in all the tested concentrations. This study on the antibacterial activity and DNA binding of Tat (49-57) is expected to provide valuable information on the mechanism of the antimicrobial activity of Tat (49-57) and could be useful for peptide drug design with highly effective bioactivity.

#### Financial assistance:

The paper was supported by the National Natural Science Foundation of China (Nos. 21572046, 21402040, 21301050).

#### Conflicts of interest:

There are no conflicts of interest.

## REFERENCES

1. Tiriveedhi V, Butko P. A fluorescence spectroscopy study on the interactions of the TAT-PTD peptide with model lipid membranes. *Biochemistry* 2007;46:3888-95.
2. Said Hassane F, Saleh AF, Abes R, Gait MJ, Lebleu B. Cell penetrating peptides: overview and applications to the delivery of oligonucleotides. *Cell Mol Life Sci* 2010;67:715-26.
3. Song J, Zhang Y, Zhang W, Chen J, Yang X, Ma P, *et al.* Cell penetrating peptide TAT can kill cancer cells via membrane disruption after attachment of camptothecin. *Peptides* 2015;63:143-9.
4. Nakase I, Tanaka G, Futaki S. Cell-penetrating peptides (CPPs) as a vector for the delivery of siRNAs into cells. *Mol Biosyst* 2013;9:855-61.
5. Presente A, Dowdy SF. PTD/CPP peptide-mediated delivery of siRNAs. *Curr Pharm Design* 2013;19:2943-7.
6. Nasrollahi SA, Fouladdel S, Taghibiglou C, Azizi E, Farboud ES. A peptide carrier for the delivery of elastin into fibroblast cells. *Int J Dermatol* 2012;51:923-9.
7. Mo RH, Zaro JL, Shen WC. Comparison of cationic and amphipathic cell penetrating peptides for siRNA delivery and efficacy. *Mol Pharm* 2011;9:299-309.
8. Xia H, Gao X, Gu G, Liu Z, Hu Q, Tu Y, *et al.* Penetrating-functionalized PEG-PLA nanoparticles for brain drug delivery. *Int J Pharm* 2012;436:840-50.
9. Rizzuti M, Nizzardo M, Zanetta C, Ramirez A, Corti S. Therapeutic applications of the cell-penetrating HIV-1 Tat peptide. *Drug Discov Today* 2015;20:76-85.
10. Brooks H, Lebleu B, Vivès E. Tat peptide-mediated cellular delivery: back to basics. *Adv Drug Deliver Rev* 2005;57:559-77.
11. Chen X, Sa'adedin F, Deme B, Rao P, Bradshaw J. Insertion of TAT peptide and perturbation of negatively charged model phospholipid bilayer revealed by neutron diffraction. *Biochim Biophys Acta* 2013;1828:1982-8.
12. Vives E, Brodin P, Lebleu B. A truncated HIV-1 Tat protein basic domain rapidly translocates through the plasma membrane and accumulates in the cell nucleus. *J Biol Chem* 1997;272:16010-7.
13. Suzuki T, Futaki S, Niwa M, Tanaka S, Ueda K, Sugiura Y. Possible existence of common internalization mechanisms among arginine-rich peptides. *J Biol Chem* 2002;277:2437-43.
14. Ziegler A, Seelig J. High affinity of the cell-penetrating peptide HIV-1 Tat-PTD for DNA. *Biochemistry* 2007;46:8138-45.
15. Hegde A H, Prashanth S N, Seetharamappa J. Interaction of antioxidant flavonoids with calf thymus DNA analyzed by spectroscopic and electrochemical methods. *J Pharm Biomed Anal* 2012;63:40-6.
16. Jung HJ, Park Y, Hahn KS. Biological activity of Tat (47–58) peptide on human pathogenic fungi. *Biochem Biophys Res Commun* 2006;345:222-8.
17. Zhao D, Ma L, Lu K. Syntheses of valpromide dipeptide derivatives and interactions of derivatives with ctDNA. *Res Chem Intermed* 2015;41:8591-601.
18. Verdon J, Berjeaud JM, Lacombe C. Characterization of anti-*Legionella* activity of warnericin RK and delta-lysin I from *Staphylococcus warneri*. *Peptides* 2008;29:978-84.
19. Jaumot J, Gargallo R. Experimental methods for studying the interactions between G-quadruplex structures and ligands. *Curr Pharm Design* 2012;18:1900-16.
20. Sirajuddin M, Ali S, Badshah A. Drug-DNA interactions and their study by UV-Visible, fluorescence spectroscopies and cyclic voltametry. *J Photochem Photobiol B* 2013;124:1-19.
21. Shi JH, Chen J, Wang J, Zhu YY. Binding interaction between sorafenib and calf thymus DNA: spectroscopic methodology, viscosity measurement and molecular docking. *Spectrochim Acta A Mol Biomol Spectrosc* 2015;136:443-50.
22. Charak S, Jangir DK, Tyagi G. Interaction studies of epirubicin with DNA using spectroscopic techniques. *J Mol Struct* 2011;1000:150-4.
23. Fuchs JE, Spitzer GM, Javed A, Biela A, Kreutz C, Wellenzohn B, *et al.* Minor groove binders and drugs targeting proteins cover complementary regions in chemical shape space. *J Chem Inf Model* 2011;51(9):2223-32.
24. Bi S, Zhang H, Qiao C, Sun Y, Liu C. Studies of interaction of emodin and DNA in the presence of ethidium bromide by spectroscopic method. *Spectrochim Acta A Mol Biomol Spectrosc* 2008;69:123-9.
25. Sahoo BK, Ghosh KS, Bera R. Studies on the interaction of diacetylcurcumin with calf thymus-DNA. *Chem Phys* 2008;351:163-9.
26. Rehman SU, Yaseen Z, Husain MA, Sarwar T, Ishqi HM, Tabish M. Interaction of 6 mercaptopurine with calf thymus DNA-deciphering the binding mode and photo-induced DNA damage. *PLoS One* 2014;9(4):e93913.
27. Sarwar T, Rehman SU, Husain MA, Ishqi HM, Tabish M. Interaction of coumarin with calf thymus DNA: deciphering the mode of binding by *in vitro* studies. *Int J Biol Macromol* 2015;73:9-16.
28. Ling X, Zhong W, Huang Q, Ni K. Spectroscopic studies on the interaction of pazufloxacin with calf thymus DNA. *J Photochem Photobiol B* 2008;3:172-6.
29. Labieniec M, Gabryelak T. Interactions of tannic acid and its derivatives (ellagic and gallic acid) with calf thymus DNA and bovine serum albumin using spectroscopic method. *J Photochem Photobiol B* 2006;2:72-8.
30. Streckowski L, Harden DB, Wydra RL, Stewart KD, Wilson WD. Molecular basis for potentiation of bleomycin-mediated degradation of DNA by polyamines. Experimental and molecular mechanical studies. *J Mol Recognit* 1989;2:158-66.
31. Deiana M, Matczyszyn K, Massin J, Olesiak-Banska J, Andraud C, Samoc M. Interactions of isophorone derivatives with DNA: spectroscopic studies. *PLoS One* 2015;10.
32. Li H, Bu X, Lu J, Xu C, Wang X, Yang X. Interaction study of ciprofloxacin with human telomeric DNA by spectroscopy and molecular docking. *Spectrochim Acta A Mol Biomol Spectrosc* 2013;107:227-34.
33. Vaidyanathan VG, Nair BU. Photooxidation of DNA by a cobalt (II) tridentate complex. *J Inorg Biochem* 2003;94:121-6.
34. Barrett MP, Gemmill CG, Suckling CJ. Minor groove binders as anti-infective agents. *Pharmacol Ther* 2013;139(1):12-23.
35. Dyatkina NB, Roberts CD, Keicher JD, Dai Y, Nadherny JP, Zhang W, *et al.* Minor groove DNA binders as antimicrobial agents. 1. Pyrrole tetraamides are potent antibacterials against vancomycin resistant Enterococci and methicillin resistant *Staphylococcus aureus*. *J Med Chem* 2002;45(4):805-17.
36. Gordon BRG, Li Y, Cote A, Weirauch MT, Ding P, Hughes TR, Liu J. Structural basis for recognition of AT-rich DNA by unrelated xenogeneic silencing proteins. *Proc Natl Acad Sci USA* 2011;108(26):10690-5.